

Biophysical Journal, Volume 114

Supplemental Information

**Simultaneous Multicolor Single-Molecule Tracking with Single-Laser
Excitation via Spectral Imaging**

**Tao Huang, Carey Phelps, Jing Wang, Li-Jung Lin, Amy Bittel, Zubenelgenubi Scott, Steven
Jacques, Summer L. Gibbs, Joe W. Gray, and Xiaolin Nan**

Supplementary Figure 1. Effect of prism orientation on spectral image quality.

Supplementary Figure 2. Superresolution imaging in 4 colors with the single-molecule spectral imaging platform.

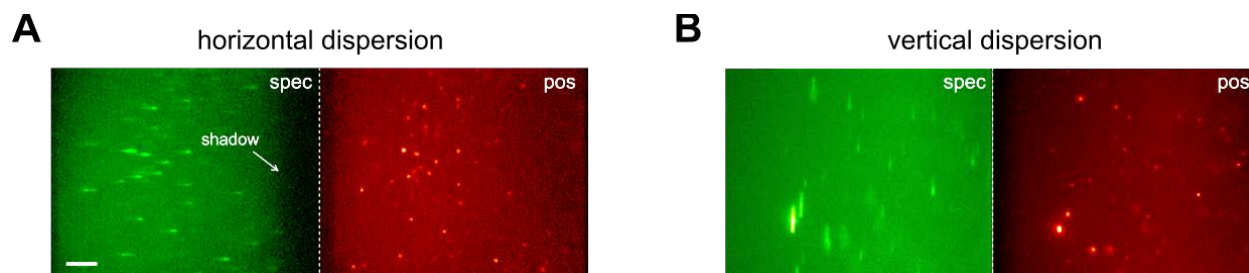
Supplementary Figure 3. Histogram of *ssd* from a 4-color single-molecule spectral imaging experiment.

Supplementary Figure 4. Resolving microtubule hollow structure with 1/3 of photons on the single-molecule spectral imaging setup.

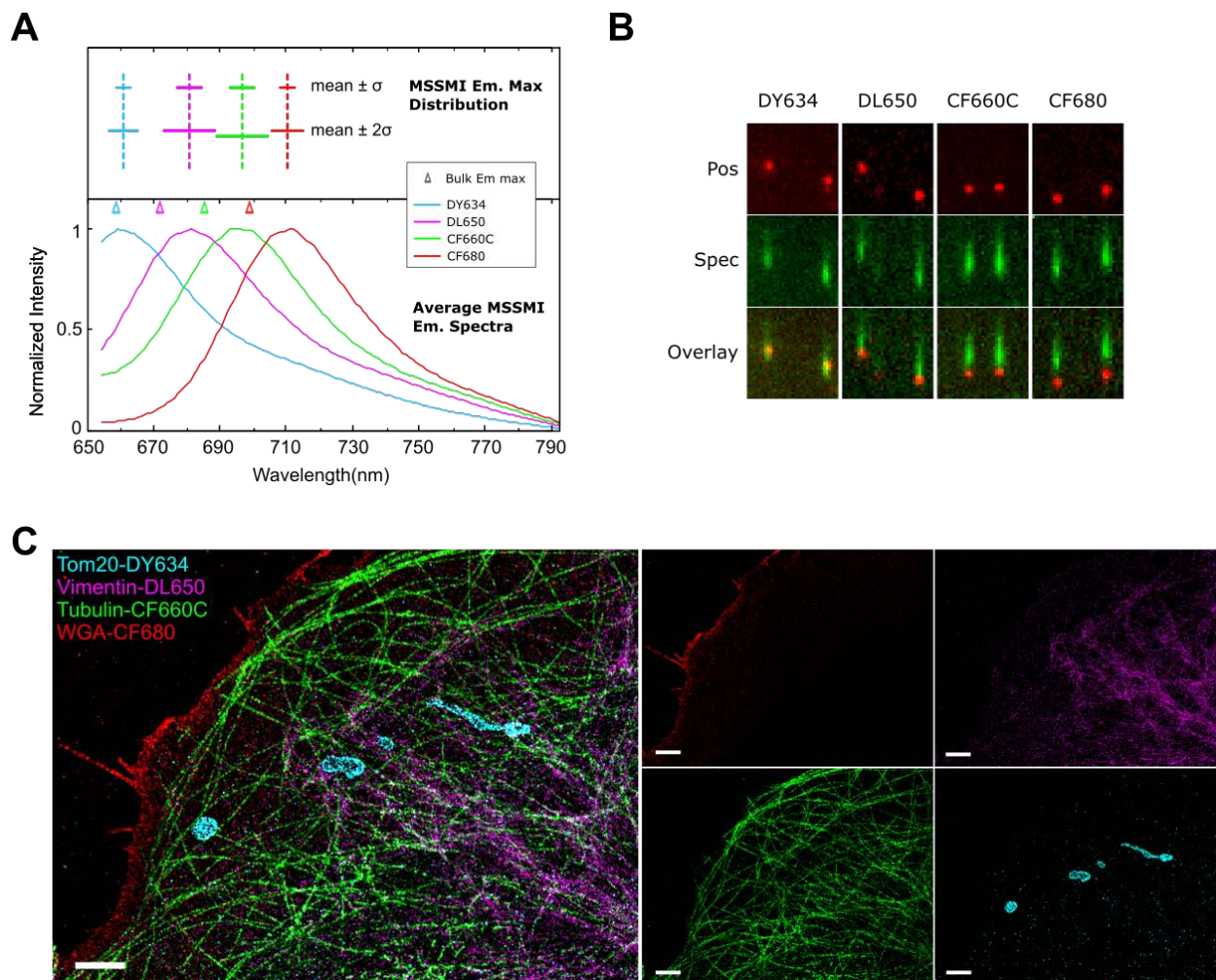
Supplementary Figure 5. SMT results with WGA-CF633, CellMask DR, and HT-CF680R.

Supplementary Figures 6-11 and text. Effects of diffusion on the measured single-molecule emission spectra

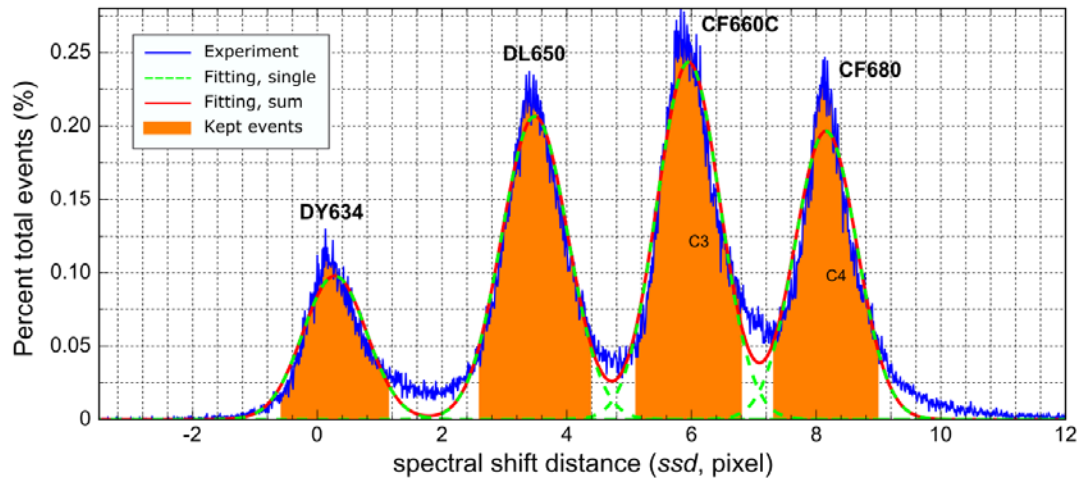
Supplementary Video 1. Raw movie for 3-color single-molecule tracking.



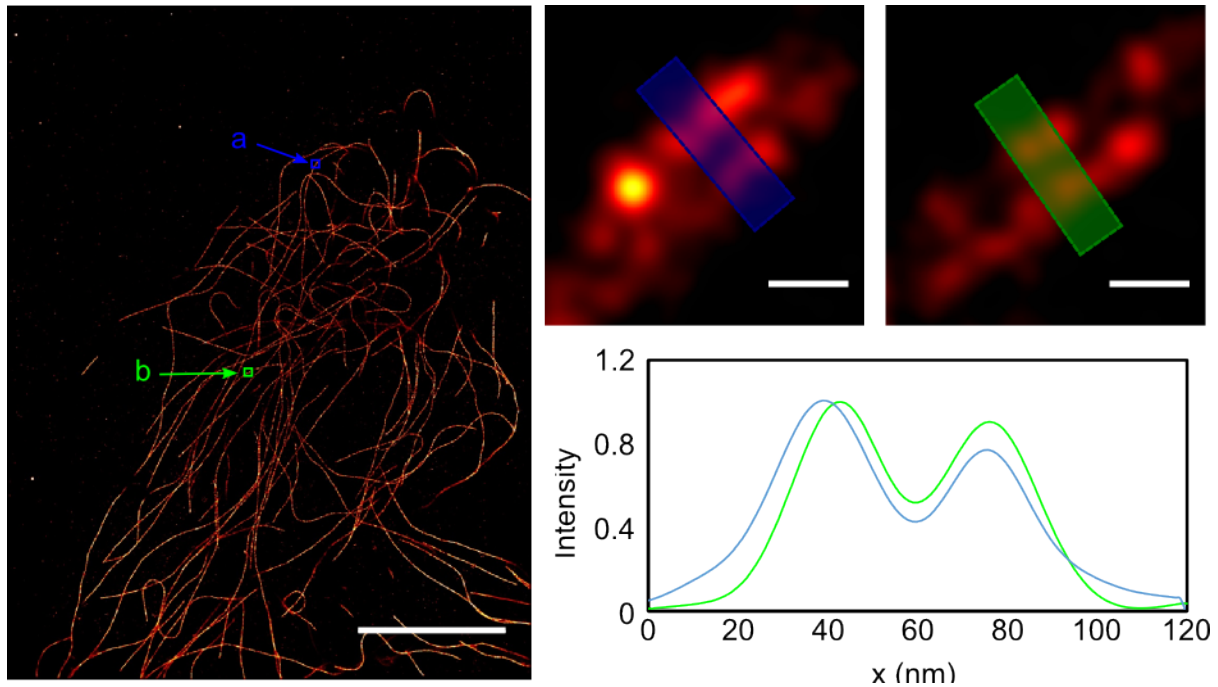
Supplementary Figure 1. Effect of prism orientation on spectral image quality. The prism can take an orientation such that the direction of light dispersion aligns with the left and right edges of the slit, resulting in ‘horizontal’ elongation of the single molecule images, where the slit edges cast shadows in the spectral channel (A), or it can be oriented to yield a ‘vertical’ dispersion where the shadows are instead casted by the top and bottom edges of the slit and are imaged outside of the field of view, hence not affecting the image quality (B). We used configuration (B) in this manuscript, as also shown in Fig. 1B.



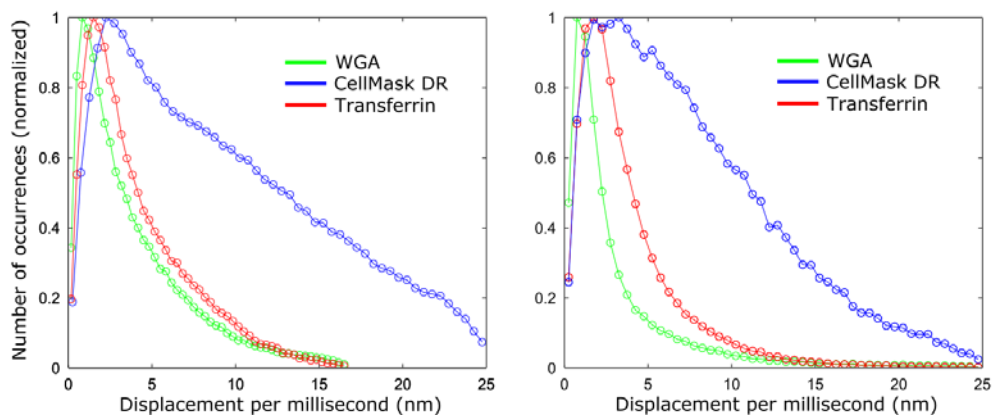
Supplementary Figure 2. Multicolor imaging of cellular structures with single-molecule spectral imaging in fixed cells. (A) Average emission spectra of DY634, DL650, CF660C, and CF680 shown in wavelength units in the lower plot, each generated by averaging the single-molecule emission spectra of $\sim 10,000$ single molecules. The upper plot shows the maximum emission wavelengths for the same four dyes measured on the spectral imaging setup, displayed as mean (vertical, dotted line) and the spread (1σ and 2σ as indicated, where σ is the standard deviation). Empty triangles mark the bulk emission wavelengths measured in solution; (B) Positional (top), spectral (middle), and overlaid (bottom) images of single DY634, DL650, CF660C, and CF680 molecules as indicated; (C) Four-color spectrally-resolved superresolution image of a U2OS cell labeled for mitochondria (Tom20, cyan), intermediate filaments (vimentin, magenta), microtubules (tubulin, green), and cell membrane (WGA, red). The overlaid image is shown on the left and images in individual channels are on the right. Scale bars, 2 μm .



Supplementary Figure 3. Histogram of *ssd* from a 4-color single-molecule spectral imaging experiment. U2OS cells were stained and imaged as described in the main text, and the measured *ssd* values for all detected localization events are plotted in the histogram. Each peak in the histogram is fitted with a Gaussian distribution (dotted green line), and the sum of all 4 Gaussians is shown in red. Based on their positions, the peaks were designated to specific fluorophores as indicated. To reduce spectral crosstalk, localization events associated with *ssd* values that fell in the border region between two adjacent peaks were discarded. Specified ranges of *ssd* values for DY634, DL650, CF660C, and CF680 were (-0.59, 1.15), (2.59, 4.39), (5.10, 6.81), (7.31, 9.00), respectively, where the first and second numbers in the brackets represent the lower and upper bounds of the *ssd* values. The resulting localization retention rates for the four fluorophores were all around 80%, and the spectral crosstalk between neighboring channels was between 0-0.7% in this case.



Supplementary Figure 4. Resolving microtubule hollow structure with 30% photons on the spectrally-resolved superresolution imaging setup. U2OS cells were labeled with rat anti- α -tubulin antibody and AF647-conjugated donkey anti-rat secondary antibody (see *Materials and Methods*) and imaged on the spectrally-resolved superresolution setup using standard STORM imaging buffer (GLOX + 100 mM MEA in PBS). Shown on the left is an overview of microtubules in a cell, with regions a (blue) and b (green) shown in zoom-in views on the top right panels. Line profiles of the boxed regions are shown in blue and green, respectively. Scale bars, 10 μ m (left) and 50 nm (right). Note that the positional channel only received \sim 30% of the photons emitted from each AF647 molecule.



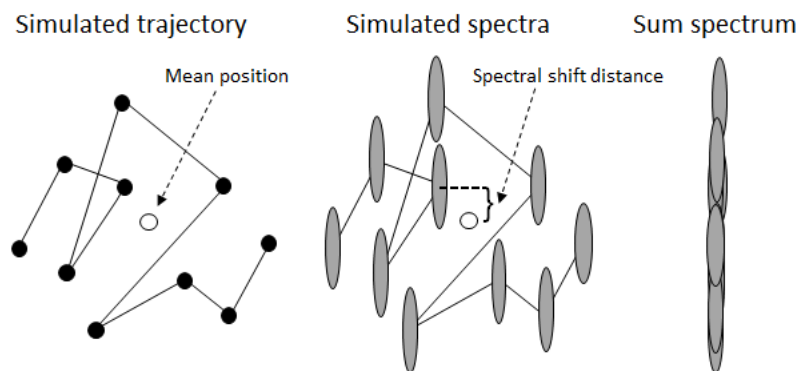
Supplementary Figure 5. SMT results of WGA-CF633, CellMask DR, and human transferrin (HT)-CF680R. Live U2OS cells were labeled with one of the three reagents and imaged on the spectral imaging setup to obtain single-molecule trajectories. The trajectories were analyzed as described previously². Both panels show histograms of calculated displacement per unit time of each molecular species with WGA-CF633 (green), CellMask DR (blue), and HT-CF680R (red) measured from the single-color (left) or 3-color single-molecule spectral imaging (right) experiments.

Effects of diffusion on the measured single-molecule emission spectra

The single-molecule spectra detected in our instrument are potentially prone to artificial broadening due to diffusive motion of the molecules. If molecules move significantly during the exposure time of the camera, the detected positions and spectra will both be motion blurred. The resulting recorded spectra could appear broader than their fixed counterparts, which could reduce the effective spectral resolution of the system and complicate identification of dye species. To determine the effect of motion blur on single-molecule spectra, we performed simulations using a home-built Matlab script. Molecular motions were simulated at a wide range of diffusion constants, and the resulting positions and spectra were calculated. We then used the peak intensity finding algorithm used in our experiments to locate the emission maximum for each molecule and determine whether motion had induced broadening and/or error in the apparent emission peak position.

Simulation Design

The simulation was performed as follows. Single-molecule trajectories were created as 2D Gaussian random walks (see Supplementary Fig. 6), with steps taken every 1 millisecond (ms), and adjustable diffusion coefficients. At each step in a trajectory, an emission spectrum was generated with finite photons. The total number of steps taken was equal to the exposure time of the camera from the experiments (i.e. 30 steps to simulate an experiment with a 30 ms exposure time). The spectra at each 1 ms step in the trajectory were summed to create the total, motion-blurred spectrum for the full, 30 ms trajectory. We used the emission spectrum of CF633 for these simulations. Before the addition of spectra at each time point was performed, each spectrum was shifted by an amount proportional to the distance traversed in the x-direction (the direction of spectral elongation) by the molecule to simulate motion blur. The mean position of the trajectory was used as the localization position. A schematic of the simulation design is shown in Supplementary Figure 6.



Supplementary Figure 6. Simulation of motion blur in molecular positions and spectra due to diffusion. Left – Single molecule trajectory. Filled circles indicate coordinates at each step in the trajectory, while the empty circle indicates the mean position, which is used as the localization position. Middle – single-molecule spectra are simulated at each time point in the random walk (here the dispersion axis, the x-axis, is displayed vertically). These spectra are shifted in space relative to the mean position. Right – the sum spectrum is the sum of all generated spectra, with each individual spectrum shifted by an amount proportional to the displacement of the particle from the mean position.

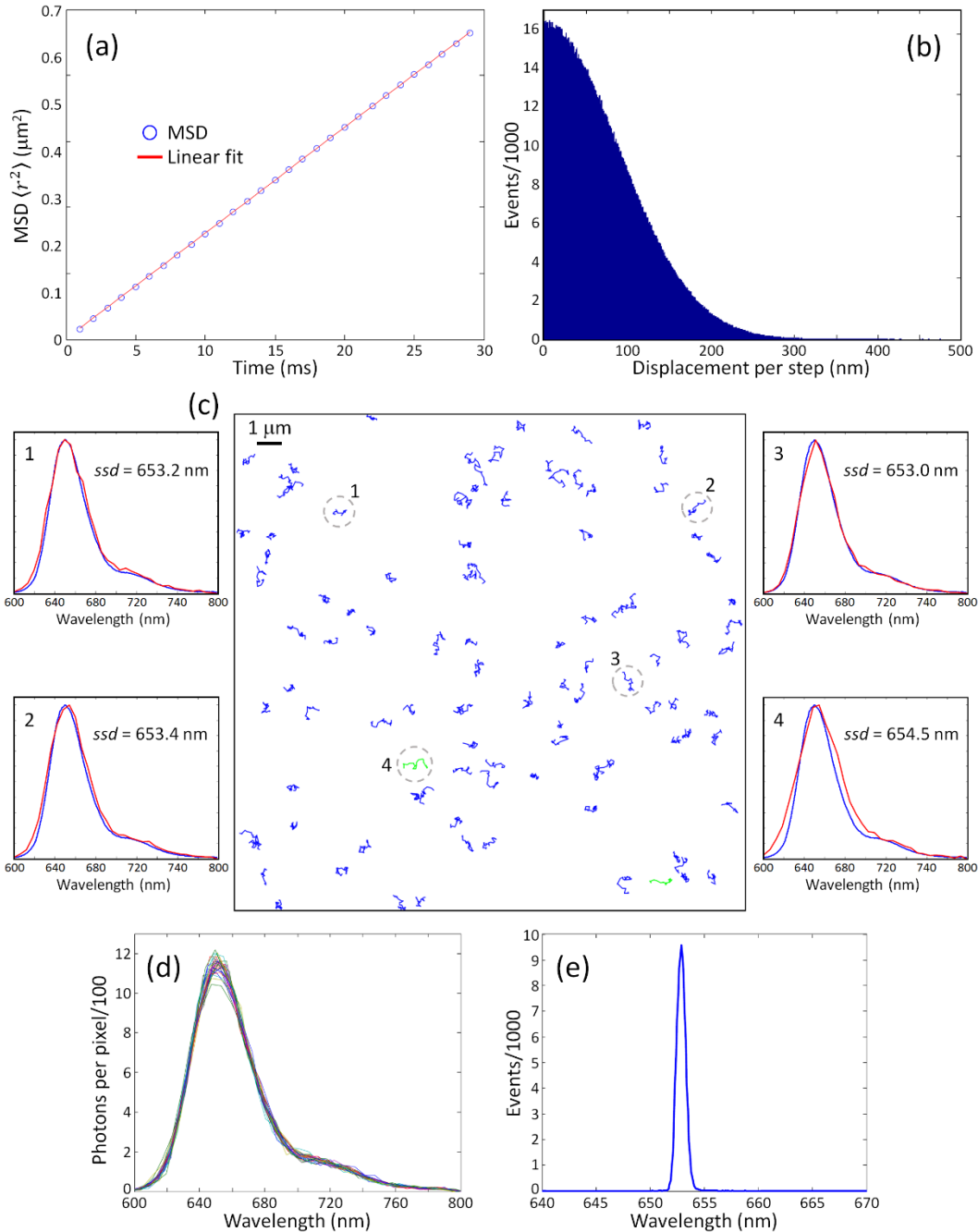
The distance that a spectrum is shifted for a given spatial displacement is determined by the optics in the experimental system. Due to the magnification of our system, each pixel on the camera corresponds to 178 nm of real space. Thus we define the conversion constant $A = 178$ nm/px. Furthermore, the spectral profile, recorded in pixel units on the camera, can be converted to spectral nanometers via calibrations described in the methods section of this manuscript. In our system, each pixel corresponds to approximately 6 nm in the spectral domain. Thus we can define the conversion constant $B = 6$ nm/px. Therefore, a molecular displacement can be related to a spectral displacement by the ratio B/A . This ratio, $6/178$, tells us that a molecular displacement of 178 nm will produce a spectral shift on the order of 6 nm in the detected spectral profile in our instrument. This ratio was used to shift the single-molecule spectra appropriately for the corresponding spatial displacements.

Simulation examples

Most of our simulations were performed in a high-photon yield regime to emphasize the effect of motion blur on spectra independently of the signal-to-noise level. We used 10,000 photons per spectrum, regardless of exposure time, and 100,000 trajectories for each set of simulation parameters. Supplementary Figures 7 and 8 demonstrate some representative results for simulations ran with diffusion coefficients $D = 2$ and $5 \mu\text{m}^2/\text{sec}$, respectively. Simulations with $D = 2 \mu\text{m}^2/\text{sec}$ are meant to represent the fastest reasonable diffusion coefficient for membrane-bound molecules, while simulations with $D = 5 \mu\text{m}^2/\text{sec}$ are shown because this diffusion coefficient marks the diffusion rate at which the effects of motion blur become significant (as will be shown). Supplementary Figures 7a and 8a show the mean square displacement (MSD) for each simulation, defined as $\text{MSD} = \langle r(t) \rangle^2$, where $r(t)$ is the distance at time t from the first coordinate in the trajectory. The MSD demonstrates that trajectories are diffusing with the desired diffusion coefficient. Supplementary Figures 7b and 8b show histograms of the displacement per. Here, the mean displacement is 71.4 and 112.8 nm for simulations with $D = 2$ and $5 \mu\text{m}^2/\text{sec}$, respectively.

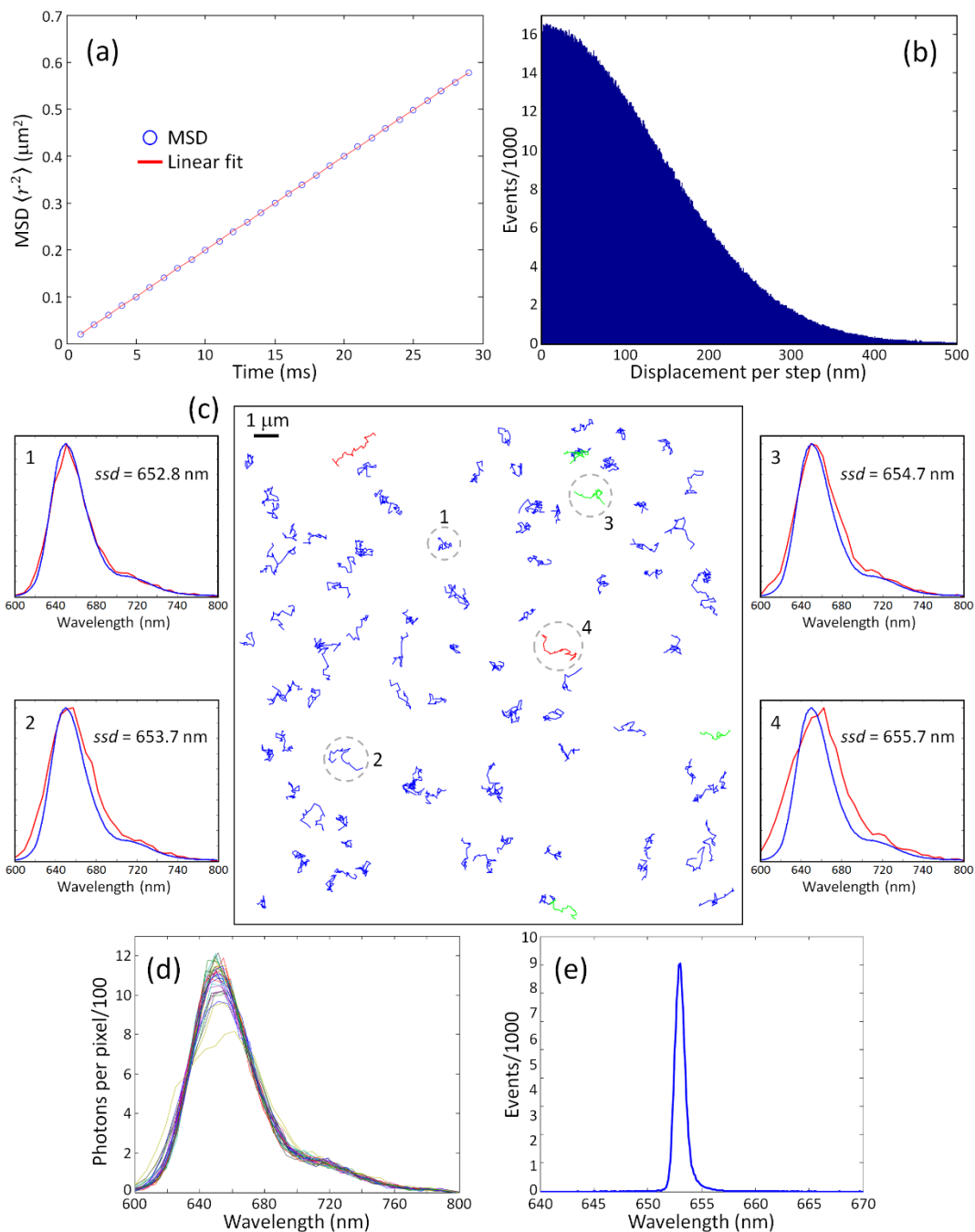
Supplementary Figures 7c and 8c show trajectory maps, each displaying a subset of 100 trajectories randomly selected from a pool of 100,000 trajectories. The trajectories are color-coded according to how closely their motion-blurred emission peak corresponds to the true value, as determined by our peak finding algorithm. Blue trajectories have less than 1 nm error, green have an error in the range 1-2 nm, and red have an error in the range 2-3 nm. No trajectories shown have greater than 3 nm error. The error is defined as the absolute value of the difference between the “correct” value (the value determined by our peak finding algorithm in fixed conditions with infinite signal) minus the observed value for each simulated trajectory. For CF633, in these simulated conditions, this is $|652.8 \text{ nm} - \text{ssd}|$, where ssd is the spectral shift distance observed for an individual single-molecule spectrum.

Some representative simulated spectra are shown to the left and right side of each trajectory map in Supplementary Figure 7c and 8c. Simulated spectra are shown in red, overlaid on the bulk spectrum in blue. Each spectrum is numbered and corresponds a circled and numbered trajectory within the map. The ssd is indicated for each spectrum, as determined by our peak finding algorithm. Supplementary Figures 7d and 8d each contain 30 random spectra overlaid onto each other. As can be seen, spectra from the $D = 2 \mu\text{m}^2/\text{sec}$ data set are mostly similar, indicating that motion blur-induced broadening has a small effect at this diffusion rate, while spectra from the $D = 5 \mu\text{m}^2/\text{sec}$ data set show more varied amplitudes and widths, indicating an increased effect of motion blur on the measured spectra. Supplementary Figures 7e and 8e show histograms of ssd values obtained for the full set of 100,000 molecules. The increased effect of motion blur in the $D = 5 \mu\text{m}^2/\text{sec}$ case is apparent by an increased standard deviation in the ssd histogram.



Supplementary Figure 7. Simulation results with a diffusion coefficient $D = 2 \mu\text{m}^2/\text{sec}$. 100,000 trajectories were simulated, with steps taken at 1 millisecond intervals for a total of 30 steps, thus simulating a 30 ms exposure time. (a) Mean square displacement (MSD) (blue circles) and a linear fit (red line). The fit has a slope $m = 8.026 \mu\text{m}^2/\text{sec}$. In 2 dimensions, this is related to the diffusion coefficient D by the formula $m = 4D$. Thus, the diffusion coefficient is $D = 2.01 \mu\text{m}^2/\text{sec}$. (b) Histogram of displacements per step. The mean displacement is 71.4 nm. (c) Trajectory map showing the diffusion path of 100 trajectories randomly selected from the total pool of 100,000 trajectories. The horizontal axis is the x-axis (dispersion direction). Trajectories are color-coded according to how accurately the motion-blurred spectra reflect the true emission peak maximum, as determined by the peak finding algorithm used in our experiments. Blue: < 1 nm error, green: 1-2 nm error. To the left and right are simulated, motion-blurred emission spectra (red) overlaid on the bulk emission spectrum of CF633 (blue). The spectra are

numbered and represent spectra for the corresponding circled and numbered trajectories in the trajectory map. The emission peak position for each motion-blurred spectrum, as determined by our peak finding algorithm, is indicated in each spectrum plot. (d) 30 randomly selected, simulated spectra are overlaid. (e) Histogram of ssd values for the entire 100,000 trajectory data set. The standard deviation is 0.42 nm.



Supplementary Figure 8. Simulation results with a diffusion coefficient $D = 5 \mu\text{m}^2/\text{sec}$. 100,000 trajectories were simulated, with steps taken at 1 millisecond intervals for a total of 30 steps, thus simulating a 30 ms exposure time. (a) Mean square displacement (MSD) (blue circles) and a linear fit (red line). The fit has a slope $m = 19.898$

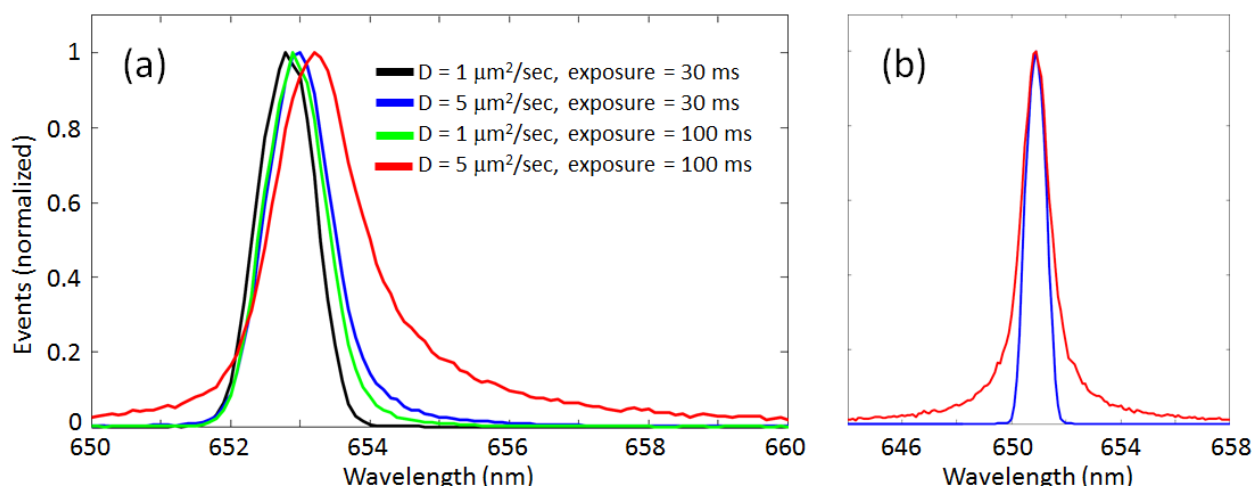
$\mu\text{m}^2/\text{sec}$, indicating the diffusion coefficient is $D = 4.97 \mu\text{m}^2/\text{sec}$. (b) Histogram of displacements per step. The mean displacement is 112.8 nm. (c) Trajectory map showing the diffusion path of 100 trajectories randomly selected from the total pool of 100,000 trajectories. The horizontal axis is the x-axis (dispersion direction). Trajectories are color-coded according to how accurately the motion-blurred spectra reflect the true emission peak maximum, as determined by the peak finding algorithm used in our experiments. Blue: < 1 nm error, green: 1-2 nm error, red: 2-3 nm error. To the left and right are simulated, motion-blurred emission spectra (red) overlaid on the bulk emission spectrum of CF633 (blue). The spectra are numbered and represent spectra for the corresponding circled and numbered trajectories in the trajectory map. The emission peak position for each motion-blurred spectrum, as determined by our peak finding algorithm, is indicated in each spectrum plot. (d) 30 randomly selected, simulated spectra are overlaid. (e) Histogram of *ssd* values for the entire 100,000 trajectory data set. The standard deviation is 0.78 nm.

As can be seen from the example spectra in these trajectory maps, trajectories with relatively small displacements along the x-axis (the dispersion axis) display spectra with negligible spectral broadening, while trajectories with a relatively large amount of propagation along the x-axis show more broadening.

Motion blur vs. diffusion coefficient and exposure time

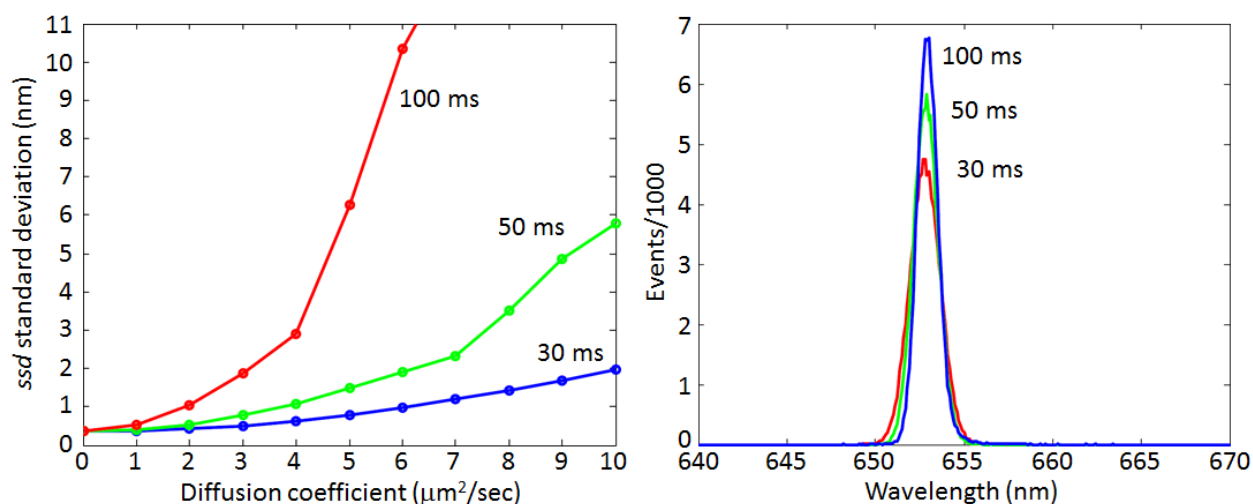
Three factors contribute to spectral broadening: (1) the optics of the single-molecule spectral imaging system, (2) the diffusion constant of the observed molecules, and (3) the exposure time of the camera. The optics of the instrument will determine how sensitive the system is to motion blur. Instruments with a higher B/A ratio will be more sensitive to motion blur, meaning they have higher magnification (i.e. smaller A), or smaller spectral dispersion (i.e. larger B). Thus the constant B/A determines how spatial displacements propagate to spectral displacements. For our system, $B/A = 0.03$. Other systems may be more or less sensitive to motion blur dependent on their optics. Thus, one should keep in mind that the results of our simulations may not directly apply to another imaging system without adjustments to this number in the simulations.

Clearly, larger diffusion constants and exposure times contribute to spectral broadening by allowing for larger displacements along the x-axis during the collection of a single-molecule spectrum. A primary aim of our simulations was to determine what diffusion constants would induce excessive motion blur in our technique, and what exposure times should be chosen to adequately minimize motion blur. Thus, we simulated 100,000 trajectories with exposure times of 30 ms and 100 ms, and diffusion constants ranging from 1-10 $\mu\text{m}^2/\text{sec}$. With each condition, we computed the *ssd* histogram that relays how accurately the emission peak maximum can be identified for the given dye species in the presence of motion blur. Supplementary Fig. 9a displays the *ssd* histogram for various conditions. As expected, the standard deviation of the *ssd* measurement is increased with increasing diffusion constant and with increased exposure time. Note, in addition to broadening, there is a slight red shift with increasing motion blur. This manifests from asymmetry in the bulk emission spectrum. To demonstrate the lack of a shift when a symmetric bulk spectrum is used, we input a Gaussian emission spectrum into the simulation and found that there was no shift associated with broadening (see Supplementary Figure 9b).



Supplementary Figure 9. (a) Histogram of *ssd* values from simulated trajectories and their associated motion blurred spectra. Each histogram is composed of 100,000 trajectories. Increased diffusion coefficients or exposure times result in an increased standard deviation of *ssd* histograms. (b) Histogram of *ssd* values when a Gaussian is used as the input spectrum, showing no red shift with increased broadening (blue: $D = 1 \mu\text{m}^2/\text{sec}$ and 30 ms exposure, red: $D = 5 \mu\text{m}^2/\text{sec}$ and 100 ms exposure). Here, the input spectrum was a Gaussian with center 651 nm and width 15.8 nm.

Supplementary Figure 10a displays the standard deviation of the *ssd* measurement for the full range of diffusion constants simulated, and for each exposure time. As shown, an exposure time of 30 ms is relatively insensitive to motion blur for the full range of diffusion constants simulated. This implies that the emission peak of membrane-bound molecules (i.e. diffusion constants typically $< 2 \mu\text{m}^2/\text{sec}$) are identified with nearly identical accuracy to immobile molecules. Furthermore, diffusion constants as high as $10 \mu\text{m}^2/\text{sec}$ show only a ~ 2 nm error in the determination of the emission peak position with this exposure time, which is smaller than the intrinsic heterogeneity of single-molecule fluorophores (2.5 nm or more in our measurements, depending on the fluorophore).



Supplementary Figure 10. Exposure time dependence on motion blur. (a) Standard deviation of emission peak maxima (*ssd*) vs. diffusion coefficient, for three exposure times (30 ms, 50, and 100 ms). Here, 10,000 photons are

used for all spectra, regardless of exposure time. 100,000 molecular trajectories were simulated with each set of parameters. (b) *ssd* histograms for three exposure times (red – 30 ms, green – 50 ms, blue – 100 ms) with diffusion constant $D = 1 \mu\text{m}^2/\text{sec}$. Here, 50 photons per millisecond are introduced, and thus larger exposure times receive larger numbers of photons per spectrum. The standard deviations are: 0.86, 0.70, and 0.64 nm for 30, 50, and 100 ms exposure, respectively.

As Supplementary Figure 10 shows, exposure times of 50-100 ms can also be used to reliably determine the emission peak for molecules with realistic diffusion constants for the vast majority of membrane-bound molecules, because the standard deviation of detected emission peak maxima remains fairly small ($< 2\text{nm}$ for molecules with diffusion constants $< 2 \mu\text{m}^2/\text{sec}$). However, the accuracy of determining the emission peak becomes rapidly error prone for diffusion constants $> 4 \mu\text{m}^2/\text{sec}$.

Increased exposure time has two competing effects. As already shown, increased exposure time will increase motion blur, and thus decrease the accuracy of the emission peak measurement. However, an increased exposure time will also provide a higher photon yield per spectral snapshot, which will provide an increased accuracy in emission peak determination. In a low motion blur regime, the benefits of a longer exposure time dominate over the decreased accuracy from motion blur. This effect is demonstrated in Supplementary Figure 10b. We set the photon yield of our trajectories to 50 photons per millisecond and used $D = 1 \mu\text{m}^2/\text{sec}$. As shown in Supplementary Figure 10a, this diffusion coefficient corresponds to low motion blur for all three exposure times. As a result, as shown in Supplementary Figure 10b, the improved accuracy in emission peak determination dominates and the *ssd* histogram becomes narrower with increased exposure time.

Summary of simulation results

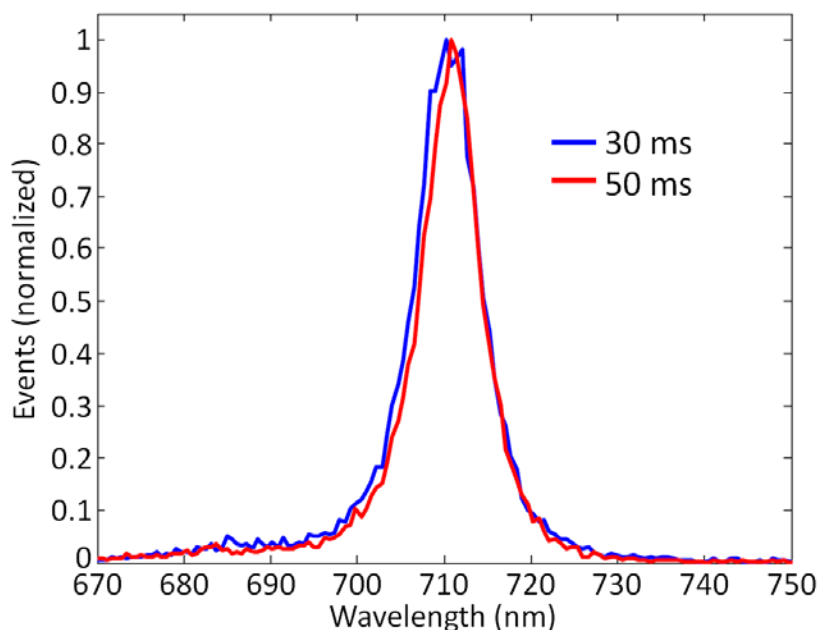
Our simulations have demonstrated that motion blur has a very small effect on single-molecule spectra in single-molecule spectral imaging measurements for typical membrane-bound molecules. Most membrane-bound molecules will diffuse at rates of $2 \mu\text{m}^2/\text{sec}$ or less. At this diffusion rate, motion blur has a negligible effect with exposure times of up to 100 ms (see Supplementary Figures 7 and 10). When measuring molecules diffusing at an even slower rate, such as those in our experiments ($0.3\text{-}0.6 \mu\text{m}^2/\text{sec}$), motion blur is even more insignificant. Other sources of noise, such as finite photon yield or spectral heterogeneity, should be given more consideration in these cases. However, if particles of interest diffuse at rates of $5 \mu\text{m}^2/\text{sec}$ or faster, one must be aware of the potential error incurred by motion blur. Motion blur can be minimized with shorter exposure times. Or alternatively, one could apply pulsed excitation to diffusing molecules, where the laser pulse is of a shorter duration than the exposure time of the camera. The motion blur incurred in such a scheme would be proportional to the pulse duration rather than the exposure time of the camera.

Our simulations highlight the effect of motion blur on single-molecule emission spectra detected by our instrument. To focus on motion blur, we have designed an idealized simulation where this effect is the most significant in terms of spectral variability from molecule to molecule. Yet some aspects of the experiment, not included in these simulations, can introduce significantly more variation between detected spectra. Firstly, we have assumed that the mean position of a trajectory corresponds to the localization position in the experiment. This may not be the case since single-molecule localization can be prone to many sources of error, including distortion of the point spread function due to motion blur. Secondly, with the exception of stochastic noise resulting from finite photons per spectrum, we did not

include sources of noise such as background light, or electronic noise. Finally, fluorophores depict heterogeneity in their spectra on the single-molecule level, typically 2.5 nm or more depending on the fluorophore. The source of this heterogeneity is not well understood, but appears to be a universal trend according to our observations.

Exposure time dependence in experiments

From our simulations, it is expected that the molecules used in our experiments, which diffuse at rates $< 1 \mu\text{m}^2/\text{sec}$, should lie in a low motion blur regime. Consistent with this notion, we found that increasing exposure times would tend to improve spectral resolution, similar to the result shown in Supplementary Figure 10b. A comparison of *ssd* histograms at two exposure times for transferrin-CF680R is shown in Supplementary Figure 11.



Supplementary Figure 11. *ssd* histograms of transferrin-CF680R, recorded at two different exposure times (blue - 30 ms, and red - 50 ms), and with the same laser power (20 mW). The standard deviations for these measurements are: 5.58 nm (30 ms) and 5.22 nm (50 ms).

The faster exposure time (30 ms) has a slightly broader *ssd* distribution than at the slower exposure time (50 ms). As our simulations have demonstrated, this is probably due to an improved single-molecule spectrum from added photon numbers, with only a negligible increase in the degree of motion blur.

Supplementary Video. Raw data frames showing single-molecule images in the spectral (left) and positional (right) channels from a live U2OS cell simultaneously labeled with CF633 (WGA), CellMask DR, and HT-CF680R.

References:

- 1 Zhang, Z., Kenny, S. J., Hauser, M., Li, W. & Xu, K. Ultrahigh-throughput single-molecule spectroscopy and spectrally resolved super-resolution microscopy. *Nat Methods* **12**, 935-938, doi:10.1038/nmeth.3528 (2015).
- 2 Nickerson, A., Huang, T., Lin, L. J. & Nan, X. Photoactivated localization microscopy with bimolecular fluorescence complementation (BiFC-PALM) for nanoscale imaging of protein-protein interactions in cells. *PLoS One* **9**, e100589, doi:10.1371/journal.pone.0100589 (2014).